Creation of a Fully Functional Cysteine-Less Variant of Osmosensor and Proton-Osmoprotectant Symporter ProP from *Escherichia coli* and Its Application to Assess the Transporter's Membrane Orientation†

Doreen E. Culham,‡ Alexander Hillar,§ James Henderson,‡ Anh Ly,‡ Yaroslava I. Vernikovska,§ Kathleen I. Racher,‡,|| Joan M. Boggs,§ and Janet M. Wood*,§

Department of Structural Biology and Biochemistry, Hospital for Sick Children, Toronto M5G 1X8 and Department of Laboratory Medicine and Pathobiology, University of Toronto, Toronto M5G 1L5, Ontario, Canada, and Department of Microbiology and Guelph-Waterloo Centre for Graduate Work in Chemistry and Biochemistry, University of Guelph, Guelph N1G 2W1, Ontario, Canada

Received June 2, 2003; Revised Manuscript Received July 24, 2003

ABSTRACT: Transporter ProP of *Escherichia coli* is an osmosensor and an osmoprotectant transporter. Previous results suggest that medium osmolality determines the proportions of ProP in active and inactive conformations. A cysteine-less (Cys-less) variant was created and characterized as a basis for structural and functional analyses based on site-directed Cys substitution and chemical labeling of ProP. Parameters describing the osmosensory and osmoprotectant transport activities of Cys-less ProP-$(His)_6$ variants were examined, including the threshold for osmotic activation and the absolute transporter activity at high osmolality (in both cells and proteoliposomes), the dependence of K_M and V_{max} for proline uptake on osmolality, and the rate constant for transporter activation in response to an osmotic upshift (in cells only). Variant ProP-$(His)_6$-C112A-C133A-C264V-C367A (designated ProP*) retained similar activities to ProP-$(His)_6$ in both cells and proteoliposomes. The bulky Val residue was favored over Ala or Ser at position 264, whereas Val strongly impaired function when placed at position 367, highlighting the importance of residues at those positions for osmosensing. In the ProP* background, variants with a single Cys residue at positions 112, 133, 241, 264, 293, or 367 retained full function. The native Cys at positions 112, 133, 264, and 367, predicted to be within transmembrane segments of ProP, were poorly reactive with membrane-impermeant thiol reagents. The reactivities of Cys at positions 241 and 293 were consistent with exposure of those residues on the cytoplasmic and periplasmic surfaces of the cytoplasmic membrane, respectively. These observations are consistent with the topology and orientation of ProP predicted by hydropathy analysis.

Living cells respond to changes in extracellular osmolality by accumulating and releasing organic osmolytes (e.g., polyols, betaines) (*1*−*6*). Osmoprotectant transporters and mechanosensitive channels mediate the uptake and release of exogenous compounds (osmoprotectants) by bacteria that are subjected to osmotic shifts (*1*, *2*, *7*−*9*). Our goal is to understand how cells sense changes in extracellular osmolality and respond by modulating the activities of osmoregulatory transporters. Recently, three osmoregulatory transporters have been purified and reconstituted in artificial membrane systems: secondary transporter ProP from *Escherichia coli* (*10*−*12*), secondary transporter BetP from *Corynebacterium glutamicum* (*13*−*15*), and ABC transporter OpuA from *Lactococcus lactis* (*16*, *17*). Each of these systems mediates compatible solute uptake at a rate determined by medium osmolality both in vivo and in vitro, facilitating further analyses of osmosensory and osmoregulatory mechanisms (*7*−*9*).

The *proP* sequence predicts a 500 amino acid protein that is a member of the major facilitator superfamily (*18*). ProP is a secondary transporter that mediates the accumulation of several structurally related organic solutes (e.g., proline, glycine betaine, ectoine) in response to increasing extracellular osmolality (*19*, *20*). It is a proton−solute symporter whose activity requires a membrane potential ($\Delta\Psi$)[1] and is further stimulated by a proton gradient (ΔpH) (*10*, *12*, *20*). Our data are consistent with a model in which osmolality determines the populations of ProP molecules in at least two states, inactive ($ProP^I$) and active ($ProP^A$) (*12*). ProP is predicted to include 11 or 12 transmembrane helices and a

† This work was supported by Research Grant OGP0000508 awarded to J.M.W. by the Natural Sciences and Engineering Research Council of Canada, Operating Grant MOP-42463 awarded to J.M.W. and J.M.B. by the Canadian Institutes for Health Research, and a Postdoctoral Fellowship awarded to A.H. by the Natural Sciences and Engineering Research Council of Canada.

* Corresponding author. Telephone: (519) 824-4120 Ext. 53866. Fax: (519) 837-1802. E-mail: jwood@uoguelph.ca.

‡ University of Guelph.

§ Hospital for Sick Children and University of Toronto.

|| Current address: Taiga Environmental Laboratory, Indian and Northern Affairs Canada, 4601 52nd Ave., Box 1500, Yellowknife X1A 2R3, NT Canada.

[1] Abbreviations: Π, osmotic pressure; $\Delta\Pi$, osmotic shift; $\Delta\Psi$, membrane potential; MOPS, 4-morpholinopropanesulfonic acid; EDTA, ethylenediamine tetraacetic acid; PEG, poly(ethylene glycol); OGM, Oregon green 488 maleimide carboxylic acid; MTSET, methanethiosulfonate-ethyltrimethylammonium.

10.1021/bi034939j CCC: $25.00
Published on Web 09/16/2003

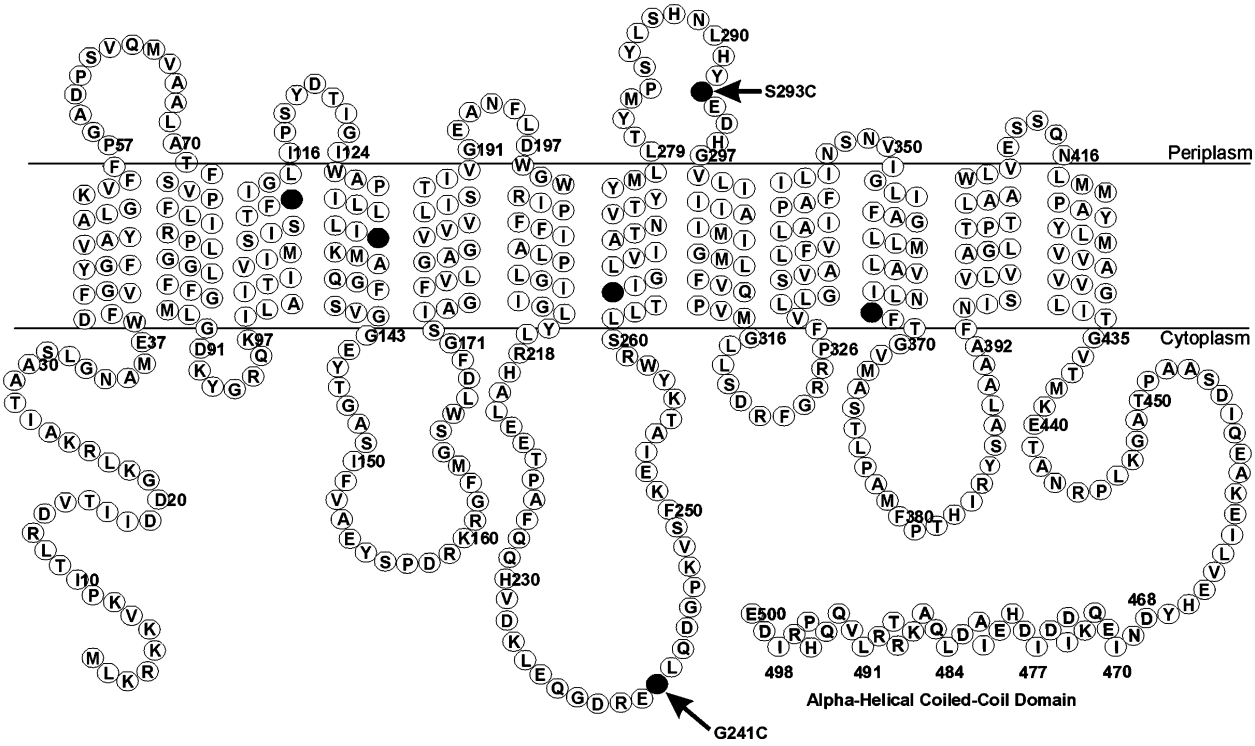

FIGURE 1: Predicted membrane topology and orientation of ProP. The membrane topology and orientation of ProP were analyzed using the algorithms discussed by Drew et al. (*35*) (TMHMM2, HMMTOP2 MEMSAT2 TOPPRED2.0, and PHD) and that described by Jayasinghe et al. (MPEx) (*36*). All algorithms predicted similar locations for putative transmembrane helices VI−XII and a cytoplasmic C-terminus. The positions of helices I−V were less obvious. TOPPRED predicted a structure that lacked transmembrane segment I and had a periplasmic N-terminus. A peptide corresponding to the C-terminal domain of ProP forms a homodimeric α-helical coiled−coil (*11*). This structure was predicted to form (*18*) with coiled−coil heptad *a* positions at I470, I477, L484, L491, and I498. Black, filled circles in the putative transmembrane segments are native Cys residues 112 (TMIII), 133 (TM IV), 264 (TMVII), and 367 (TMX). Other filled circles represent G241 and S293, each of which was replaced with a Cys.

cytoplasmic C-terminus (Figure 1). A peptide replica of the carboxyl terminal domain of ProP forms a homodimeric α-helical coiled−coil in vitro (*11*). To date, the proportions of $ProP^I$ and $ProP^A$ have been inferred from changes in the catalytic activity of ProP-$(His)_6$ (*10*, *12*, *21*). While this indirect approach has yielded useful information, it is now essential to test the structural model of ProP (Figure 1) and directly monitor any conformational changes that are associated with osmosensing.

Secondary transporters are refractory to crystallization and structure determination via NMR spectroscopy. Alternative techniques have therefore been developed for structure−function analysis of these integral membrane proteins (*22*). The creation of functional cysteine-less (Cys-less) variants followed by site-directed Cys replacement has proven particularly fruitful. Introduced Cys residues provide sites for directed labeling, paving the way for experiments that can reveal membrane topology and orientation in cells and proteoliposomes as well as structural and dynamic changes (*23*, *24*).

This paper describes the creation of a cysteine-less ProP-$(His)_6$ variant, ProP*, that is fully functional as an osmosensor and a secondary transporter both in vivo and in vitro. Characterization of multiple transporter variants en route to the creation of ProP* revealed that the amino acids at positions 264 and 367 are important to osmosensing by ProP-$(His)_6$. ProP* now serves as a platform for the introduction of cysteine residues at new locations within the protein. We report here that the native Cys at positions 112, 133, 264, and 367 are poorly reactive with membrane-impermeant thiol reagents, consistent with their putative location in transmembrane domains. The reactivities of Cys introduced at positions 241 and 293 are consistent with cytoplasmic and periplasmic localizations of those residues, respectively. These observations support predictions based on hydropathy analysis of the ProP sequence (Figure 1).

EXPERIMENTAL PROCEDURES

Materials and Culture Media. E. coli phospholipids (polar lipid extract, acetone/ether washed) were purchased from Avanti Polar Lipids, Inc. (Alabaster, AL). Dodecyl β-D-maltoside and Triton X-100 were purchased from Anatrace (Maumee, OH). *N*-Octyl-1-β-D-glucoside was purchased from Calbiochem (San Diego, CA). Oregon green 488 maleimide carboxylic acid (OGM) was purchased from Molecular Probes Inc. (Eugene, OR), and methanethiosulfonate ethyltrimethylammonium (MTSET) was purchased from Toronto Research Chemicals Inc. (Toronto, ON). OGM and MTSET were prepared as stock solutions in *N*,*N*-dimethylformamide (Fisher Scientific Inc., Nepean, ON) and stored at −20 °C, protected from light, prior to use. Egg white lysozyme (UltraPure grade) was obtained from Caledon Laboratories (Georgetown, ON). Bovine pancreatic DNase I (type II) was from Boehringer-Mannheim (Laval, PQ). Ampicillin, imidazole, L-arabinose, and β-mercaptoethanol were from Sigma Chemical Co. (St. Louis, MO). Other reagents were of the highest grade available. Buffers were prepared as described by Racher et al. (*12*), and solution osmolalities were measured with a Wescor vapor pressure osmometer (Wescor, Logan, UT). Bacteria were cultivated

in LB (*25*) or in NaCl-free MOPS medium, a variant of the MOPS medium described by Neidhardt et al. (*26*) from which all NaCl had been omitted. This base medium was supplemented with NH_4Cl (9.5 mM) as a nitrogen source and glycerol (0.4% (v/v)) as a carbon source. L-Tryptophan (245 μM) and thiamine hydrocholoride (1 μg/mL) were added to meet auxotrophic requirements to create a complete growth medium with an osmolality of 0.12 mol/kg. Ampicillin (50 μg/mL) was added as required to maintain plasmids based on vector pBAD24.

Bacteria, Plasmids, and Molecular Biological Manipulations. Both *proP* expression and ProP activity are osmoregulated (*27*). To focus on the osmoregulation of transporter activity in vivo, genes encoding ProP variants (ProP-$(His)_6$ and its variants) were expressed in an osmolality-independent manner from the AraC-controlled P_{BAD} promoter (*11*). The same system allowed us to overexpress and purify ProP-$(His)_6$ for reconstitution with the *E. coli* lipid, forming proteoliposomes (*10*, *12*). ProP-$(His)_6$ and its variants were expressed by plasmid-bearing derivatives of *E. coli* WG350 (F^- *trp lacZ rpsL thi* Δ(*putPA*)*101* Δ(*proU*)*600* Δ(*proP-melAB*)*212*) (*18*). Each strain contained plasmid pDC80 (a derivative of vector pBAD24 (*28*) in which expression of *proP-(His)$_6$* is controlled by the arabinose-inducible P_{BAD} promoter (*11*)) or a derivative of that plasmid encoding the specified ProP-$(His)_6$ variant.

Plasmids encoding ProP-$(His)_6$ variants were created by site-directed mutagenesis essentially according to the Stratagene QuikChange Site-Directed Mutagenesis procedure with *Pwo* DNA polymerase from Boehringer Mannheim (Laval, PQ) and *DpnI* restriction endonuclease from New England Biolabs (Mississauga, ON). No mineral oil overlay was used, and amplified DNA was transformed into DH5α competent cells (F^- ϕ80 d*lacZ*ΔM15 Δ(*lacZYA-argF*)U169 *recA1 endA1 hsdR17* (r_k^- m_k^+) *supE44* λ^- *thi-1 gyrA relA1*) (*29*). Oligonucleotide primers were designed to both introduce the desired amino acid change and to create an additional restriction endonuclease recognition site, thereby facilitating both screening of putative mutants and routine testing of bacterial cultures. Transformants were selected on LB plates supplemented with ampicillin (100 μg/mL), and extracted DNA was screened for the appropriate REN site alterations. The sequence of the entire *proP* gene in each mutant was determined by the Laboratory Services Division, University of Guelph, and appropriate plasmids were introduced to *E. coli* WG350 for subsequent experimentation.

Transport Assays: Intact Bacteria and Proteoliposomes. Bacteria were cultivated in NaCl-free MOPS medium (*21*), ProP-$(His)_6$ was purified, proteoliposomes were prepared (*10*), proline uptake rates were measured and analyzed (*21*), and the expression levels of ProP-$(His)_6$ and its variants in intact bacteria were determined (*11*) as previously described, except that an anti-His-HRP conjugate (Qiagen Inc., Mississauga, ON) was used to detect expression of ProP-$(His)_6$ and its variants. To determine the rate of activation of ProP-$(His)_6$ and ProP-$(His)_6$-AAVA in response to an osmotic upshift, bacteria expressing those transporters were cultivated, washed, and resuspended in NaCl-free MOPS medium supplemented with 50 mM NaCl (0.24 mol/kg). The initial rate of proline uptake was determined at a series of times after the bacteria were introduced to an assay medium based on NaCl-free MOPS medium supplemented with 0.2 M NaCl, and the resulting data were analyzed as described by Milner et al. (*30*).

Site-Directed Fluorescence Labeling. Appropriate *E. coli* strains were grown as 5 mL overnight precultures in LB broth at 37 °C. The preculture was used to inoculate a 50 mL volume of LB (1%, v/v). Following 1 h incubation at 37 °C with aeration, the culture was induced by the addition of L-arabinose to a final concentration of 0.2%, and the culture was further incubated for 2−3 h. Three 12-mL aliquots of cells were harvested by centrifugation (12 000 rpm, 2 min) in microcentrifuge tubes.

Washing and labeling were carried out as described by Ye et al. (*31*), with minor modifications. Briefly, all three aliquots were washed with buffer A (100 mM K sulfate, 50 mM K phosphate, pH 8.0). Aliquot one was labeled only on the cell surface. It was resuspended in 4 mL of buffer A plus OGM (40 μM), incubated for 15 min at room temperature, and quenched with β-mercaptoethanol (2 mM). In aliquot two, residues on the cell surface were blocked with MTSET. This sample was resuspended in buffer A plus MTSET (2 mM) and incubated for 10 min at room temperature. Both of the above aliquots were then washed, pelleted by centrifugation, and resuspended three times using buffer B (100 mM K sulfate, 50 mM MOPS-K, pH 7.0). All three aliquots of cells were then resuspended in a lysis solution consisting of egg white lysozyme (300 μg/mL), DNase I (40 μg/mL), EDTA (5 mM), and Tris-HCl (10 mM, pH 7.5) and incubated at room temperature for 15 min. Lysis was completed by diluting 2 mL of each aliquot into 18 mL of distilled water in a 30-mL Corex centrifuge tube on ice. Aliquots were centrifuged for 10 min in a JA20 rotor (Beckman) at 7000 rpm, and the pellet was washed with ice cold water, centrifuged, and resuspended another two times to prepare the membrane fraction. The membranes recovered from the second and third aliquots were resuspended in buffer C (20 mM K phosphate, 40 μM OGM, pH 8.0). These aliquots were incubated for 15 min at room temperature and frozen (dry ice/ethanol bath) and thawed three times. The reactions were quenched with mercaptoethanol as above. In this way, either the previously inaccessible cytoplasmic face (for the second aliquot) or both cytoplasmic and periplasmic faces (for the third aliquot) of the cell membranes could be labeled by OGM. The membranes were washed with ice cold water three times as described previously. All three aliquots were resuspended by extensive vortex mixing in 3 mL of a solubilization buffer described previously (*10*, *32*). Following resuspension, 200 μL of a Ni^{2+}−nitrilotriacetic acid resin (Ni−NTA Superflow, Qiagen Inc., Santa Clarita, CA) was added to each tube, the tubes were incubated overnight at 4 °C on a rotator, the resulting mixtures were poured into spin minicolumns (MicroBioSpin, Bio-Rad Inc., Hercules, CA), and they were spun for 10 min in a microcentrifuge to remove the resuspension buffer. The resin matrix was then washed three times with 0.5-mL aliquots of wash buffer (solubilization buffer supplemented with 200 mM NaF and 50 mM imidazole) (10−15 min, 12 000 rpm). Each ProP* variant was then eluted with 100 μL of 50 mM Tris/HCl, 2% SDS, 10% glycerol, 0.5 M imidazole, pH 7.0. Eluted samples were immediately analyzed by denaturing SDS−PAGE by loading 20-μL aliquots in triplicate onto 12 or 14% gels. Each gel was repeated. Following electrophoresis, band fluorescence was determined by exposure to UV light using

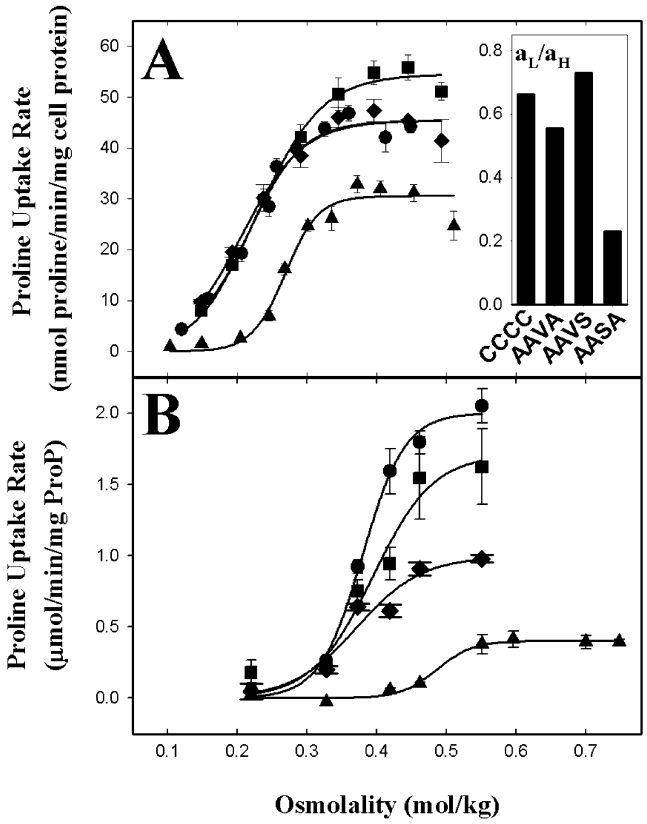

FIGURE 2: Impact of assay medium osmolality on proline uptake via ProP-$(His)_6$ and its cysteine-less variants in intact bacteria (A) and proteoliposomes (B). Proline uptake via ProP-$(His)_6$ and its variants was measured as described in Experimental Procedures using NaCl to adjust the osmolalities of the transport assay media. Circles, ProP-$(His)_6$; squares, ProP-$(His)_6$-AAVA; diamonds, ProP-$(His)_6$-AAVS; triangles, ProP-$(His)_6$-AASA. Inset to panel A: ratio of the proline uptake activity of each ProP-$(His)_6$ variant measured in assay medium with 0.05 M NaCl (0.24 mol/kg) to that measured in assay medium with 0.17 M NaCl (0.49 mol/kg) (a_L/a_H).

a UVP gel documentation platform (DiaMed Laboratory Supplies Inc., Mississauga, ON) with a CCD camera attachment and a Macintosh based data capture and analysis program (UVP Grab-It). Each gel was also stained for protein using Coomassie Brilliant Blue and imaged using a white light source. Band intensities on the gels were determined by densitometry using the image analysis routines supplied with the UVP Grab-It program. The density values for the triplicate lanes were averaged and used to calculate the ratio of UV fluorescence to protein recovered. The ratios from two different gels were averaged to give the mean ± range reported in Figure 7. Each experiment was repeated once using a second set of membranes. Similar results were obtained in both experiments.

To compare OGM labeling of ProP* variants in membranes with that in SDS solution, two aliquots of cells were processed as follows. For OGM labeling of ProP* variants in membranes, one aliquot was treated as described above (cell aliquot three). For OGM labeling in SDS solution, a second aliquot was treated by the same procedure to and including the lysis step. Recovered membrane ghosts were immediately solubilized, and ProP* variants were purified and eluted from Micro-BioSpin columns in SDS-containing elution buffer as described above. OGM labeling was then carried out by adding 1 μL of stock OGM solution to 10 μL of recovered ProP protein in elution buffer as described (*33*) (OGM concentration approximately 1 mM, less than 10% final DMF concentration). Samples were mixed directly in the pipet tips and allowed to incubate for 10 min at room temperature. One μL of 1.4 M β-mercaptoethanol was added to the samples to quench the labeling reaction, all samples were immediately subjected to SDS−PAGE, and the resulting gels were analyzed to determine fluorescence and protein content as described previously. Because of variations in fluorescence from one experiment to another, all samples for which fluorescence/protein ratios were compared were labeled and analyzed at the same time.

RESULTS

Characterization of ProP-$(His)_6$ Activity: Criteria for Retention of Full Function by Cysteine-Less ProP-$(His)_6$. The osmoprotectant uptake activity of transporter ProP-$(His)_6$ is a sigmoid function of assay medium osmolality that can be

Table 1: Osmolality Responses of ProP-$(His)_6$ Variants

variant[a]	osmolyte[b]	material[c]	osmolality response parameter[d]		
			A_{max}	$\Pi_{1/2}/RT$	B
ProP-$(His)_6$	NaCl	Cells	45.4 ± 1.1	0.214 ± 0.004	0.039 ± 0.004
	NaCl	PRLs	2.00 ± 0.08	0.380 ± 0.005	0.030 ± 0.005
	glucose	PRLs	1.77 ± 0.12	0.399 ± 0.009	0.022 ± 0.006
ProP-$(His)_6$-AAVA	NaCl	Cells	54.5 ± 1.3	0.230 ± 0.006	0.046 ± 0.005
	NaCl	PRLs	1.71 ± 0.21	0.395 ± 0.018	0.043 ± 0.015
	glucose	PRLs	1.05 ± 0.14	0.436 ± 0.017	0.029 ± 0.011
ProP-$(His)_6$-AAVS	NaCl	Cells	45.4 ± 1.3	0.206 ± 0.007	0.044 ± 0.007
	NaCl	PRLs	1.00 ± 0.07	0.372 ± 0.012	0.047 ± 0.011
	glucose	PRLs	0.94 ± 0.15	0.406 ± 0.025	0.055 ± 0.018
ProP-$(His)_6$-AASA	NaCl	Cells	30.6 ± 0.8	0.269 ± 0.004	0.024 ± 0.004
	NaCl	PRLs	0.40 ± 0.02	0.487 ± 0.014	0.026 ± 0.010

[a] ProP-$(His)_6$ variants are described using the nomenclature ProP-$(His)_6$-XXXX, where the Xs represent the amino acid replacements at the positions occupied by Cys in the native protein (positions 112, 133, 264, and 367). [b] Proline uptake was measured as described in Experimental Procedures using 200 μM proline as substrate with NaCl or D-glucose (as indicated) to adjust the osmolality of the assay medium. [c] Bacteria were cultivated in NaCl-free MOPS medium (0.12 mol/kg) and prepared for the transport assay as described. Two or more replicate experiments were performed, and representative data are shown. Proteoliposomes (PRLs) were prepared using the indicated ProP-$(His)_6$ variant as described in Experimental Procedures. Data are representative of three PRL preparations for ProP-$(His)_6$, two for ProP-$(His)_6$-AAVA, one for ProP-$(His)_6$-AAVS, and three for ProP-$(His)_6$-AASA. [d] The osmolality response parameters (and errors in those parameters) were computed by fitting the initial rate of proline uptake (a_0) and the osmolality of the transport assay medium (Π/RT) to eq 1 using nonlinear regression as previously described (*21*). Units of the osmolality response parameters are A_{max}, nmol/min/mg of cell protein for cells and μmol/min/mg of ProP for proteoliposomes; $\Pi_{1/2}/RT$, mol/kg; and B, mol/kg.

characterized by the following empirical relationship:

$$a_0 = A_{max}[1 + \exp - (\Pi - \Pi_{1/2})/RTB]^{-1} \qquad (1)$$

where Π is the osmotic pressure of the transport assay medium, a_0 is the initial rate of proline uptake measured with medium of osmolality Π/RT, A_{max} is the uptake rate that would be observed at infinite medium osmolality (nmol/min/mg of cell protein for cells and μmol/min/mg of ProP for proteoliposomes), R is the gas constant, T is the temperature, $\Pi_{1/2}/RT$ is the medium osmolality yielding half-maximal ProP-(His)$_6$ activity (mol/kg), and B is a constant inversely related to the slope of the response curve (mol/kg) (this relationship is illustrated for ProP-(His)$_6$ in Figure 2 (black circles)). For reasons discussed by Culham et al. (*21*), qualitatively similar relationships between a_0 and Π/RT are observed with intact bacteria and proteoliposomes, but the absolute values of parameters A_{max}, $\Pi_{1/2}/RT$, and B in vivo and in vitro are different (compare Figure 2, panels A and B; Table 1).

The goal of this research was to construct a cysteine-less (Cys-less) derivative of ProP-(His)$_6$ for which these parameters matched those of the parent transporter as closely as possible, both in vivo and in vitro. Transporter mutants were created and screened in vivo to assess whether their thresholds for osmotic activation (expressed above as $\Pi_{1/2}/RT$) and their absolute activities (expressed above as A_{max}) were comparable to those of ProP-(His)$_6$. Bacteria expressing the transporter variants were cultivated in NaCl-free MOPS medium (osmolality 0.12 mol/kg), and their proline uptake activities were measured in assay media supplemented with 50 or 170 mM NaCl (osmolalities 0.24 and 0.49 mol/kg, respectively). The ratio of these proline uptake activities (a_L/a_H) is exquisitely sensitive to changes in the magnitude of $\Pi_{1/2}/RT$, increases and decreases in $\Pi_{1/2}/RT$ being manifest as dramatic decreases and increases in a_L/a_H, respectively (see inset to Figure 2A). The absolute value of the uptake rate in the latter medium (a_H) is a good indicator of the maximum activity attainable (unless, of course, there is also a dramatic increase in the osmolality required to activate the transporter). Transporters that met the criteria of minimal perturbation to these parameters were then characterized in greater detail using both intact bacteria and proteoliposomes.

Impact of Cysteine Replacements on ProP-(His)$_6$ Activity in Bacteria. Transporter ProP has Cys residues at positions 112, 133, 264, and 367. Transporter variants are described using the nomenclature ProP-(His)$_6$-XXXX, where the Xs represent the single letter codes for the amino acids occupying those four positions. For example, ProP-(His)$_6$-AAVA is ProP-(His)$_6$-C112A-C133A-C264V-C367A. Replacement of C112 or C133 with Ala had little impact on transporter activity (as indicated by a_H, Figure 3A) or osmolality response (a_L/a_H, Figure 3B), whereas replacement of C264 or C367 with Ala, Ser, or Val was more perturbing. In an effort to create a fully functional, Cys-less ProP-(His)$_6$ variant, residues 264 and 367 were replaced with Ala, Ser, or Val in a variety of combinations with Ala in positions 112 and 133. Each of the constructed Cys-less variants was expressed at a level indistinguishable from that of ProP-(His)$_6$ (data not shown). As anticipated, transporter activity (a_H, Figure 4A) and osmolality response (a_L/a_H, Figure 4B) were again particularly sensitive to replacements at positions 264 and 367. The bulky Val residue was deleterious to transporter activity in position 367 and favorable to transporter activity in position 264. Variants ProP-(His)$_6$-AAVA and ProP-(His)$_6$-AAVS were selected as most similar in transporter activity and osmolality response to the parent, ProP-(His)$_6$. They were analyzed further with variant ProP-(His)$_6$-AASA, for which both a_H and a_L/a_H were lower than those of ProP-(His)$_6$, as a comparator.

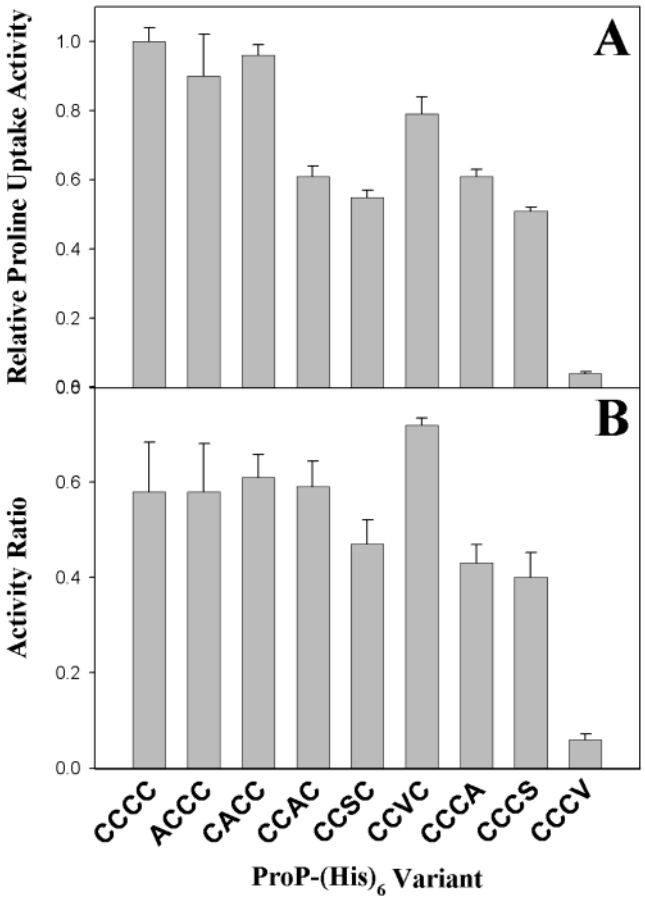

FIGURE 3: Proline uptake activities of ProP-(His)$_6$ derivatives in which individual Cys residues are replaced. Bacteria were cultivated in NaCl-free MOPS medium without or with 0.12 M NaCl. NaCl supplementation of the growth medium in this range does not alter the proline uptake activity due to ProP-(His)$_6$ in these media (*21*). Transport assays were conducted as described in Experimental Procedures using assay media supplemented with 0.05 and 0.17 M NaCl. (A) The proline uptake activity of the transporter variant in a transport assay medium supplemented with 0.17 M NaCl (a_H) relative to that of ProP-(His)$_6$ measured in the same way during the same experiment. (B) The ratio of the proline uptake activity of each ProP-(His)$_6$ variant measured in assay medium with 0.05 M NaCl to that measured in assay medium with 0.17 M NaCl (a_L/a_H). For the nine replicate cultures of bacteria expressing ProP-His$_6$ that were used to obtain data represented by Figures 3, 4, and 6 of this paper, the proline uptake activities measured at low and high osmolality (a_L and a_H) were 35 ± 8 and 54 ± 12 nmol/min/mg of protein, respectively.

Detailed Examination of Cys-Less ProP-(His)$_6$ Variants. The activities of the candidate Cys-less ProP-(His)$_6$ derivatives were characterized in greater detail. In intact bacteria, each yielded an osmotic activation profile and parameters similar to those of ProP-(His)$_6$ (see Figure 2A, squares and diamonds for ProP-(His)$_6$-AAVA and ProP-(His)$_6$-AAVS, respectively, and Table 1). In contrast, the threshold for osmotic activation of Cys-less variant ProP-(His)$_6$-AASA

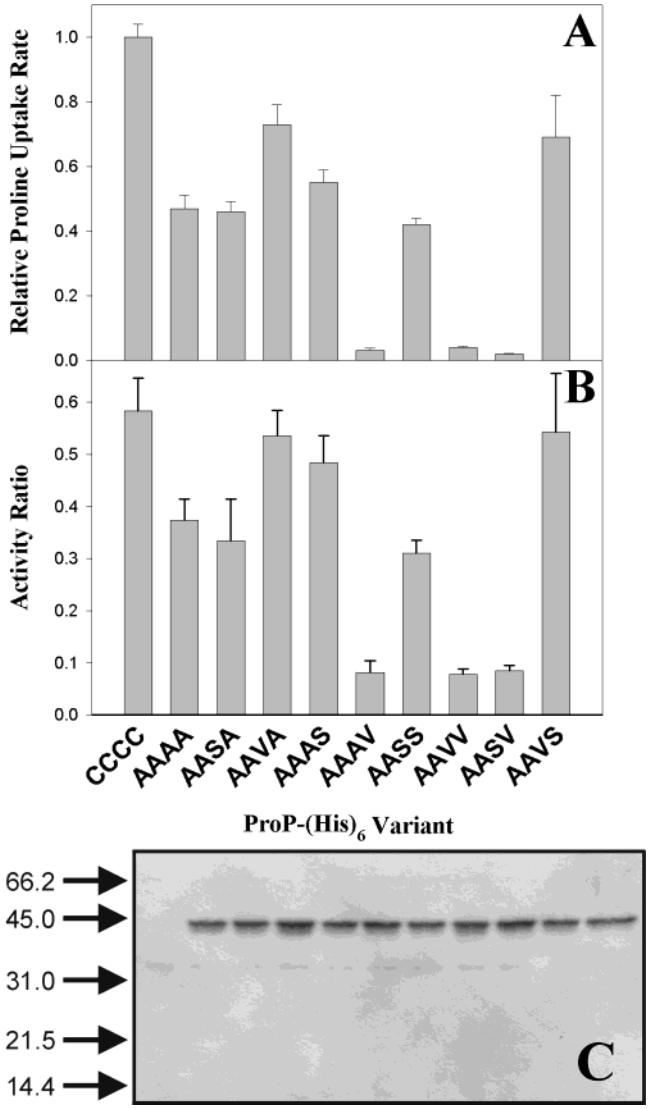

FIGURE 4: Proline uptake activities of Cys-less ProP-$(His)_6$ derivatives. Bacteria were cultivated in NaCl-free MOPS medium without or with 0.12 M NaCl, and transport assays were conducted as described in Experimental Procedures using assay media supplemented with 0.05 and 0.17 M NaCl. NaCl supplementation of the growth medium in this range does not alter the proline uptake activity due to ProP-$(His)_6$ in these media. (A) The proline uptake activity of the transporter variant in a transport assay medium supplemented with 0.17 M NaCl (a_H) relative to that of ProP-$(His)_6$ measured in the same way during the same experiment. (B) The ratio of the proline uptake activity of each ProP-$(His)_6$ variant measured in assay medium with 0.05 M NaCl (0.24 mol/kg) to that measured in assay medium with 0.17 M NaCl (0.49 mol/kg) (a_L/a_H). For the nine replicate cultures of bacteria expressing ProP-His_6 that were used to obtain data represented by Figures 3, 4, and 6 of this paper, the proline uptake activities measured at low and high osmolality (a_L and a_H) were 35 ± 8 and 54 ± 12 nmol/min/mg protein, respectively. (C) Western blot illustrating the relative expression levels of the Cys-less ProP-$(His)_6$ variants in whole cell extracts. The first lane contained an extract from vector control bacteria (WG350 pBAD24) not expressing ProP. The other lanes contained extracts from bacteria expressing the Cys-less ProP-$(His)_6$ variants in the same order as for panels A and B. The heavy band with an electrophoretic mobility corresponding to 45 kDa corresponds to purified ProP-$(His)_6$.

was dramatically elevated, and the activity attained was dramatically reduced, again emphasizing the sensitivity of both the activity and the osmolality response of the transporter to amino acid changes at positions 264 and 367

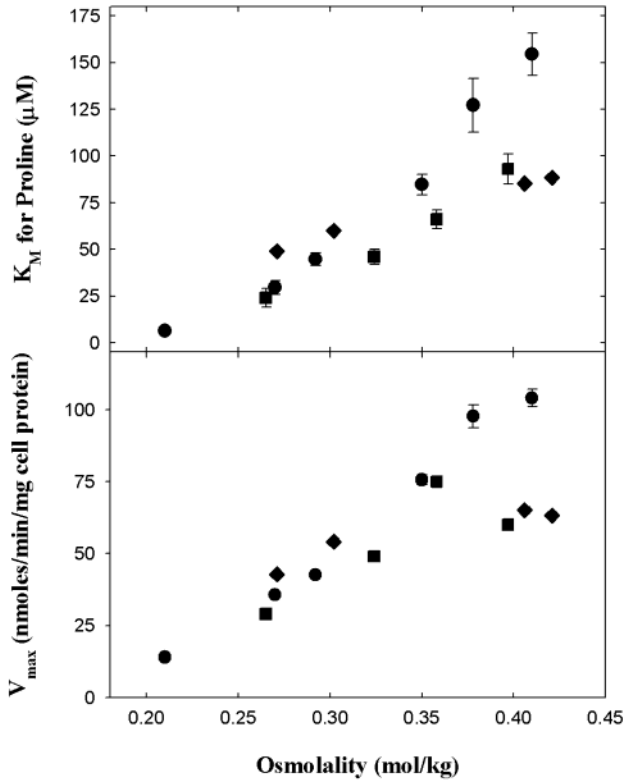

FIGURE 5: Kinetics of proline uptake via ProP-$(His)_6$ and its Cys-less variants. The appropriate *E. coli* strains were cultivated, washed, and resuspended in NaCl-free MOPS minimal medium that has an osmolality of 0.12 mol/kg. The initial rate of proline uptake was measured as described in Experimental Procedures using assay media adjusted with NaCl to the indicated osmolalities and radiolabeled proline at an appropriate series of concentrations (11−900 μM). K_M for proline and V_{max} were determined at each osmolality by nonlinear regression using the Michaelis−Menten equation as model. The data for ProP-$(His)_6$ (circles) are derived from Figure 4 of Culham et al. (*21*). The Cys-less variants included ProP-$(His)_6$-AAVA (squares) and ProP-$(His)_6$-AAVS (diamonds).

(Figure 2A, triangles, and Table 1).

The activities of ProP-$(His)_6$, ProP-$(His)_6$-AAVA, and ProP-$(His)_6$-AAVS in intact bacteria were similar functions of osmolality when proline uptake activity was measured at a single proline concentration (200 μM, Figure 2A). Both the K_M of ProP-$(His)_6$ for proline and the transporter V_{max} increase as assay medium osmolality increases (*21*). K_M and V_{max} were less osmolality dependent for ProP-$(His)_6$-AAVA and ProP-$(His)_6$-AAVS (Figure 5, squares and diamonds, respectively) than for ProP-$(His)_6$ (Figure 5, black circles). However, these differences were not deemed sufficiently large to preclude further experimentation employing these Cys-less variants. The half-time for the activation of ProP-$(His)_6$-AAVA in cells subjected to an osmotic upshift (0.24 to 0.53 mol/kg) was 1.3 min, a value similar to those previously reported for the activation of ProP (approximately 1 min) (*30*, *34*).

The activities of candidate Cys-less ProP-$(His)_6$ derivatives were also examined after purification and reconstitution in proteoliposomes (Figure 2B). Once again, variants ProP-$(His)_6$-AAVA and ProP-$(His)_6$-AAVS had similar osmotic activation profiles (Figure 2B, squares and diamonds, respectively) and parameters (Table 1) to ProP-$(His)_6$. In proteoliposomes, even more than in intact cells, the osmolality threshold for the activation of ProP-$(His)_6$-AASA was

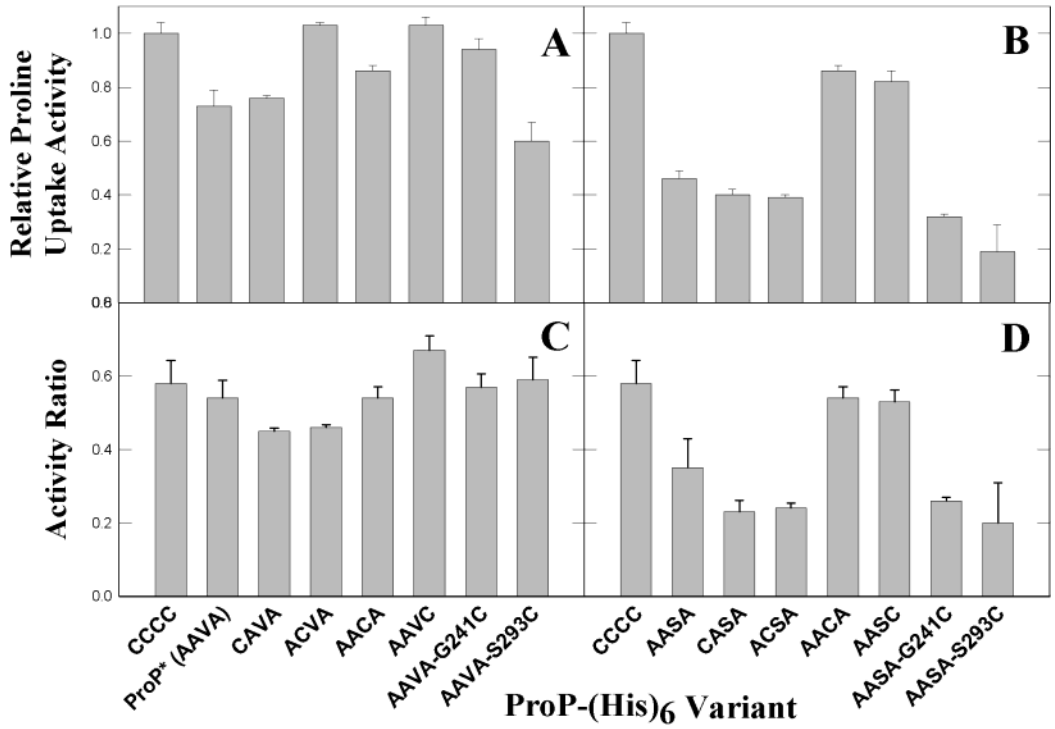

FIGURE 6: Proline uptake activities of ProP-(His)$_6$ derivatives retaining single Cys residues. Bacteria were cultivated, and transport assays were conducted as described in Experimental Procedures and the legend for Figure 3. Panels A and B: proline uptake activity of the transporter variant in a transport assay medium supplemented with 0.17 M NaCl (a_H) relative to that of ProP-(His)$_6$ measured in the same way during the same experiment. Panel A: Cys-less variant ProP* (or AAVA) and its derivatives compared to ProP-His$_6$ (CCCC). Panel B: Cys-less variant AASA and its derivatives. Panels C and D: ratio of the proline uptake activity of each ProP-(His)$_6$ variant measured in an assay medium with 0.05 M NaCl (0.24 mol/kg) to that measured in an assay medium with 0.17 M NaCl (0.49 mol/kg) (a_L/a_H). Panel C: Cys-less variant ProP* (or AAVA) and its derivatives as compared to ProP-His$_6$ (CCCC). Panel D: Cys-less variant AASA and its derivatives. For the nine replicate cultures of bacteria expressing ProP-His$_6$ that were used to obtain data represented by Figures 3, 4, and 6 of this paper, the proline uptake activities measured at low and high osmolality (a_L and a_H) were 35 ± 8 and 54 ± 12 nmol/min/mg of protein, respectively.

dramatically increased, and its maximal activity (A_{max}) was significantly reduced, reinforcing the importance of the amino acid residue at position 264 for osmosensing (Figure 2B, triangles).

Characteristics of ProP Derivatives Harboring Single Cys Residues. ProP variants that harbored single Cys residues were created in the backgrounds of ProP-(His)$_6$-AAVA and ProP-(His)$_6$-AASA. They included transporters retaining one of the Cys present in wild-type ProP (positions 112, 133, 264, and 367) and transporters with Cys replacing Gly241 or Ser293. The activities (a_H) and osmolality responses (a_L/a_H) of the variants prepared in the ProP-(His)$_6$-AAVA background were comparable to those of ProP-(His)$_6$, whereas the corresponding properties of mutants prepared in the ProP-(His)$_6$-AASA background were consistently low (Figure 6). On the basis of these experiments, ProP-(His)$_6$-AAVA was selected as the Cys-less variant to be used as a platform for further amino acid replacements, and it was designated ProP* to simplify subsequent nomenclature.

Membrane Topology and Orientation of ProP.* The experiments described previously validated the use of single Cys strains based on ProP* to study ProP structure−function relations. Site-directed fluorescence labeling, using the fluorescent probe OGM coupled with the blocking agent MTSET, was used to test our model for the orientation and topology of ProP. Maloney and co-workers have used this method to probe the topology and transmembrane domain interfaces of various regions of the oxalate/formate transporter of *Oxalobacter formigenes* (*31*, *33*). Both OGM and MTSET are membrane impermeant reagents that react with cysteine thiols, but only OGM is fluorescent. OGM labels periplasmic Cys residues in intact cells, but it should label cytoplasmic Cys residues only after cell lysis. If intact cells are treated with MTSET before membrane preparation by cell lysis, subsequent treatment with OGM labels only cytoplasmic Cys residues. In ProP*, the target Cys were predicted to reside within transmembrane helices (C112, C133, C264, and C367), in a cytoplasmic loop (G241C) or in a periplasmic loop (S293C) (Figure 1).

No OGM fluorescence was associated with ProP* from intact cells (Figure 7, uppermost panel, lane 1, left). However, substantial background fluorescence was detected when the probe was used on membranes obtained following lysis of the cells, regardless of whether MTSET had been used to block reactive residues on the external surface of the cells (Figure 7, uppermost panel, lanes 2 and 3, left, respectively). It is likely this was due to modification of lysine residues on the cytoplasmic-facing surface of ProP*. Maleimides are known to react with amines at pH values above 7.5 (the labeling pH was 8), and lysine residues are predicted to occur only in large loops or long N- or C-terminal domains (>30 residues) on the cytoplasmic surface of ProP (Figure 1). We attempted to reduce this background by labeling at a pH of 7.4 or 7.0, but the resultant fluorescence recovered was not significantly altered (results not shown). In the case of OxlT, for which OGM labeling yields little or no background

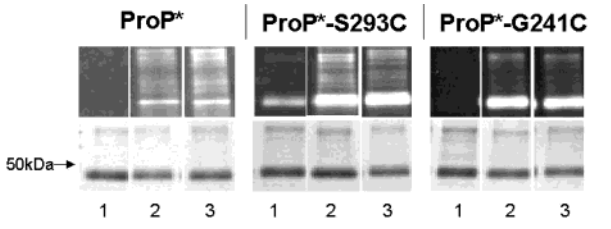

ProP-His Variant	External OGM	MTSET Block/ Internal OGM	External+Internal OGM
Cys-less	0	0.33 ± 0.03	0.33 ± 0.02
S293C	0.14 ± 0.04	0.36 ± 0.12	0.60 ± 0.04
G241C	0	0.51 ± 0.06	0.53 ± 0.04

FIGURE 7: Cysteine 293 and 241 are on the periplasmic and cytosolic membrane surfaces, respectively. OGM labeling, MTSET blocking, recovery of labeled protein by Ni−NTA chromatography, SDS−PAGE, and visualization of the resulting gels were conducted as described in Experimental Procedures. The topmost panels show fluorescence, and the middle panels show Coomassie Blue staining of the same SDS−PAGE gels. Lane 1: intact cells were labeled externally with OGM. Lane 2: cells were labeled externally with MTSET, followed by lysis and labeling of freeze−thawed membranes by OGM. Lane 3: cell membranes were labeled with OGM with no prior MTSET blocking. The position of the 50 kDa protein standard is indicated by the arrow on the left side of the figure. The table at the bottom of the figure gives the fluorescence-to-protein ratios determined for a typical experiment by densitometry as the mean ± range for duplicate gels, each run in triplicate.

fluorescence, there are six fewer lysine residues, and they occur in loops that are generally much shorter than those predicted for ProP.

OGM/MTSET labeling of variants Cys*-S293C and Cys*-G241C yielded different results (Figure 7). ProP*-S293C was labeled in intact cells by OGM (uppermost panel, lane 1, center), while ProP*-G241C was not (uppermost panel, lane 1, right). The ratios of fluorescence to protein recovered (bottom of Figure 7) indicate that external MTSET added to intact cells reduced OGM labeling of protein in membranes from cells expressing ProP*-C293 but not from those expressing ProP*-G241C (compare External + Internal OGM with MTSET Block/Internal OGM). These results are consistent with the exposure of Cys293 in the periplasm and Cys 241 on the cytoplasmic side of the membrane. The residual labeling not blocked by MTSET is probably due to OGM labeling of lysines on the cytoplasmic side. OGM labeling was also used to determine Cys accessibility in ProP* variants harboring a single native Cys residue or all four native Cys residues. This was done by comparing the labeling of those residues in the membrane-associated and the SDS-solubilized transporters. These ProP* variants were labeled with much lower efficiencies than C241 or C293 (Table 2), as might be expected if the wild-type Cys are in sterically restricted environments within the membrane. All of these data are consistent with the proposed membrane topology and orientation of ProP (Figure 1).

Table 2: Labeling Efficiencies of Cys Residues in ProP* Variants

ProP variant[a]	labeling efficiency (membranes/SDS)[b]
ProP-$(His)_6$	0.45 ± 0.12
ProP*-G241C	1.01 ± 0.04
ProP*-S293C	0.91 ± 0.07
CAVA	0.58 ± 0.16
ACVA	0.54 ± 0.26
AACA	0.50 ± 0.14
AAVC	0.65 ± 0.12

[a] Terminology as used in Table 1 and Figures 1 and 7 and as described in the text. [b] Ratio of Oregon green maleimide labeling of ProP variants in membranes relative to that in the SDS-solubilized protein. Labeling is determined as fluorescence per amount of protein as analyzed by densitometry of UV fluorescence and Coomassie Blue staining of the same gel, following SDS−PAGE. All samples were analyzed in duplicate. Values are the means ± standard deviation for three or more culture samples. The same trend toward a greater labeling efficiency of G241C and S293C relative to wild-type ProP-$(His)_6$, CAVA, ACVA, AACA, or AAVC was observed in all experiments done for each variant. The labeling efficiency of ProP* was 1, indicating a high accessibility of the lysines that also contributes significantly to the labeling in all of these variants, as indicated in Figure 7.

DISCUSSION

Transporter ProP of *E. coli* is both an osmosensor and an osmoregulatory transporter. Water flows out across the phospholipid-based membrane when the osmolality of the medium bathing cells or proteoliposomes is increased with membrane-impermeant osmolytes. Experiments performed with intact bacteria and with proteoliposomes containing purified ProP-$(His)_6$ indicate that ProP responds to osmotically induced changes in the composition of the cytoplasm or proteoliposome lumen (*10*, *12*, *21*). The data are consistent with a model in which the transporter can exist in inactive and catalytically active conformations. Studies in progress will define the solution properties that modulate transporter conformation and the mechanism(s) by which they act.

To date, the rate of proline uptake via ProP has been used as an indicator of the protein's osmosensory response. Although the impact of variables related to this catalytic activity on measurements of osmosensing can be minimized (*12*), it would be preferable to directly monitor protein conformational changes associated with osmosensing. Here, we report the construction and characterization of transporter ProP* (ProP-$(His)_6$-C112A-C133A-C264V-C367A), a His-tagged, Cys-less ProP derivative that will serve as a platform for site-directed labeling with chromophores that can report changes in ProP conformation in response to osmotic perturbations. Osmosensing and osmoregulatory proline transport via ProP* have been characterized in terms of the osmolality required for half-maximal transporter activity ($\Pi_{1/2}/RT$), the transporter activity that would be attained at infinite medium osmolality (A_{max}), the osmolality-dependent kinetics of proline uptake (K_M and V_{max}), and the half-time for the activation of the transporter in response to an osmotic upshift in both cells and proteoliposomes (Figure 2, Table 1, Figure 5, and text). Since these parameters are very similar for ProP* and ProP-$(His)_6$, we can be confident that information obtained through experimentation with ProP* will faithfully represent the properties of the native protein.

In the course of these studies, we found that although the four wild-type Cys were not required for activity, the nature of the amino acids at positions 264 and 367 were critical for osmosensing by ProP. In particular, the absolute transporter activity was significantly reduced, and the osmolality required to attain half-maximal transporter activity ($\Pi_{1/2}/RT$) was significantly elevated if Ala or Ser rather than Val

replaced Cys at position 264. Conversely, Ala was preferred over Ser, which was preferred over Val as replacements for the Cys at position 367, with Val at position 264 (Figures 2−6, Table 1).

Analysis of the ProP sequence using Internet-based topology prediction algorithms (*35*, *36*) suggests that ProP includes 11 or 12 transmembrane α-helices and a cytoplasmic C-terminus (Figure 1). C264 and C367 are both predicted to be near the cytoplasm−membrane interface, within transmembrane segments. These results suggest that the packing of amino acid side chains in this region of the protein is important and that placement of probes in this region may yield further insights regarding conformational changes related to osmosensing.

We have exploited ProP* by testing the transporter topology and orientation predicted by hydropathy analysis. Replacement of Gly241 or Ser293 with Cys did not alter ProP* activity (Figure 6, note that ProP* is labeled AAVA in this figure). The patterns of labeling of ProP*-G241C and ProP*-S293C with fluorescent maleimide OGM and blocking by MTSET in intact cells and membrane fractions were consistent with the predicted localization of these residues in the cytoplasm and periplasm, respectively. The carboxyl terminus of ProP is known to be cytoplasmic (*37*) (Culham and Wood, unpublished data). Wild-type Cys112, Cys133, Cys264, and Cys367 of ProP* in membranes were only partially accessible to OGM, while Cys241 and Cys293 were completely accessible. This is consistent with the location of the former in transmembrane domains. These results validate the C-terminal half of the predicted, 12 transmembrane helix model, but further experimentation will be required to thoroughly test it, particularly to determine whether ProP possesses 11 or 12 transmembrane helices and whether its N-terminus is cytoplasmic or periplasmic.

ACKNOWLEDGMENT

We are grateful to Shannon Pochailo and Anne-Marie Pelletier for assistance with the construction and characterization of cysteine-less ProP-$(His)_6$ variants and to Monica Pearson and Petra Bochtler for predictions of the membrane topology and orientation of ProP.

REFERENCES

1. Wood, J. M. (1999) *Microbiol. Mol. Biol. Rev. 63*, 230−262.
2. Booth, I. R., and Louis, P. (1999) *Curr. Opin. Microbiol. 2*, 166−169.
3. Burg, M. B. (1997) *Curr. Opin. Nephrol. Hypertens. 6*, 430−433.
4. Perlman, D. F., and Goldstein, L. (1999) *J. Exp. Zool. 283*, 725−733.
5. Rontein, D., Basset, G., and Hanson, A. D. (2002) *Metab. Eng. 4*, 49−56.
6. Barbier-Brygoo, H., Vinauger, M., Colcombet, J., Ephritikhine, G., Frachisse, J., and Maurel, C. (2000) *Biochim. Biophys. Acta 1465*, 199−218.
7. Poolman, B., Blount, P., Folgering, J. H. A., Friesen, R. H. E., Moe, P. C., and van der Heide, T. (2002) *Mol. Microbiol. 44*, 889−902.
8. Morbach, S., and Krämer, R. (2002) *ChemBioChem 3*, 384−397.
9. Wood, J. M., Bremer, E., Csonka, L. N., Krämer, R., Poolman, B., van der Heide, T., and Smith, L. T. (2001) *Comp. Biochem. Physiol. 130*, 437−460.
10. Racher, K. I., Voegele, R. T., Marshall, E. V., Culham, D. E., Wood, J. M., Jung, H., Bacon, M., Cairns, M. T., Ferguson, S. M., Liang, W.-J., Henderson, P. J. F., White, G., and Hallett, F. R. (1999) *Biochemistry 38*, 1676−1684.
11. Culham, D. E., Tripet, B., Racher, K. I., Voegele, R. T., Hodges, R. S., and Wood, J. M. (2000) *J. Mol. Recog. 13*, 1−14.
12. Racher, K. I., Culham, D. E., and Wood, J. M. (2001) *Biochemistry 40*, 7324−7333.
13. Ruebenhagen, R., Roensch, H., Jung, H., Kraemer, R., and Morbach, S. (2000) *J. Biol. Chem. 275*, 735−741.
14. Rübenhagen, R., Morbach, S., and Krämer, R. (2001) *EMBO J. 20*, 5412−5420.
15. Peter, H., Burkovski, A., and Krämer, R. (1998) *J. Biol. Chem. 273*, 2567−2574.
16. van der Heide, T., and Poolman, B. (2000) *Proc. Natl. Acad. Sci. U.S.A. 97*, 7102−7106.
17. van der Heide, T., Stuart, M. C. A., and Poolman, B. (2001) *EMBO J. 20*, 7022−7032.
18. Culham, D. E., Lasby, B., Marangoni, A. G., Milner, J. L., Steer, B. A., van Nues, R. W., and Wood, J. M. (1993) *J. Mol. Biol. 229*, 268−276.
19. Grothe, S., Krogsrud, R. L., McClellan, D. J., Milner, J. L., and Wood, J. M. (1986) *J. Bacteriol. 166*, 253−259.
20. MacMillan, S. V., Alexander, D. A., Culham, D. E., Kunte, H. J., Marshall, E. V., Rochon, D., and Wood, J. M. (1999) *Biochim. Biophys. Acta 1420*, 30−44.
21. Culham, D. E., Henderson, J., Crane, R. A., and Wood, J. M. (2003) *Biochem. 42*, 410−420.
22. Kaback, H. R., Sahin-Toth, M., and Weinglass, A. B. (2001) *Nat. Rev. Mol. Cell Biol. 2*, 610−620.
23. Hubbell, W. L., Cafiso, D. S., and Altenbach, C. (2000) *Nat. Struct. Biology 7*, 735−739.
24. Columbus, L., and Hubbell, W. L. (2002) *Trends Biochem. Sci. 27*, 288−295.
25. Miller, J. H. (1972) *Experiments in Molecular Genetics*, Cold Spring Harbor Laboratory, Cold Spring Harbor, NY.
26. Neidhardt, F. C., Bloch, P. L., and Smith, D. F. (1974) *J. Bacteriol. 119*, 736−747.
27. Kempf, B., and Bremer, E. (1998) *Arch. Microbiol. 170*, 319−330.
28. Guzman, L.-M., Belin, D., Carson, M. J., and Beckwith, J. (1995) *J. Bacteriol. 177*, 4121−4130.
29. Hanahan, D. (1983) *J. Mol. Biol. 166*, 557−569.
30. Milner, J. L., Grothe, S., and Wood, J. M. (1988) *J. Biol. Chem. 263*, 14900−14905.
31. Ye, L., Jia, Z., Jung, T., and Maloney, P. C. (2001) *J. Bacteriol. 183*, 2490−2496.
32. Jung, H., Tebbe, S., Schmid, R., and Jung, K. (1998) *Biochem. 37*, 11083−11088.
33. Fu, D., and Maloney, P. C. (1998) *J. Biol. Chem. 273*, 17962−17967.
34. Kunte, H. J., Crane, R. A., Culham, D. E., Richmond, D., and Wood, J. M. (1999) *J. Bacteriol. 181*, 1537−1543.
35. Drew, D., Sjöstrand, D., Nilsson, J., Urbig, T., Chin, C., de Gier, J. W., and von Heinje, G. (2002) *Proc. Natl. Acad. Sci. U.S.A. 99*, 2690−2695.
36. Jayasinghe, S., Hristova, K., and White, S. H. (2001) *J. Mol. Biol. 312*, 927−934.
37. Marshall, E. V. Osmoregulation of ProP: elucidating the roles of the ion coupling, Ph.D. Thesis, University of Guelph, 1996.

BI034939J